African Journal of Pure & Applied Sciences

ISSN: 2710-0758
DOI: https://doi.org/10.33886/ajpas.v5i2.568

Journal homepage: http://journal.ku.ac.ke/index.php/AJPAS

Research Article Open Access

Exploring the Efficacy and Suitability of Infrared Sensors at 940nm and 1150nm Wavelengths for Non-Invasive Glucose Monitoring: A Comparative Study

Kirui Julius[1], Munji Mathew[2], Ochoo Lawrence[2], Nyenge Raphael[2*], Okumu John[2]

[1*]Department of Biological and Physical sciences, Karatina University

[2*]Department of Physics, Kenyatta University

Corresponding author email address:nyenge.raphael@.ku.ac.ke

Received 16th July, 2024: Accepted 9th October 2024; Published online: 20th December 2024

How to Cite:

Kirui , J., Munji , M., Ochoo , L., Nyenge, R., & Okumu , J. Exploring the Efficacy and Suitability of Infrared Sensors at 940nm and 1150nm Wavelengths for Non-Invasive Glucose Monitoring: A Comparative Study. *African Journal of Pure and Applied Sciences, 5(2).* https://doi.org/10.33886/ajpas.v5i2.568

ABSTRACT

The changing lifestyle has resulted in the rise of the high prevalence of diabetes globally. Patients diagnosed with diabetes need to constantly keep track of their sugar levels. This is widely used so that necessary action can be taken to correct insulin deviation. The current invasive and minimally invasive methods used are useful, but expensive and prone to pain and infections. As a remedy, non-invasive methods are preferred. Among non-invasive methods, is the use of NIR technique. This give promising results, pain-free, free from infections and the method is cheap. The study comparatively investigates 940nm and 1150nm IR sensors to determine and ascertain their efficacy and suitability for monitoring glucose. The study used 940nm LED, and 1150nm IR LED independently as transmitters, and two photodiodes each with spectral wavelength range from 900nm to 1700nm for sensing. The current-to-voltage amplifier, a filter, amplification, and linearization circuit were implemented using an LM358 op amp together with a combination of resistors and capacitors. Fifteen samples of glucose concentration were prepared for testing taking into account the same environmental conditions.

In both 940nm and 1150nm IR sensors, a change in glucose concentration give a voltage output. The water absorbance with the 1150nm sensor is high when compared with that of the 940nm sensor which is minimal. The efficacy of the two sensors as per Clarke Error Grid analysis are within the required ranges of region A and B, therefore suitable for monitoring glucose non-invasively. The degree of accuracy as per Bland Altman is about 93% for the two sensors. The residual plots indicate appropriate regression lines for the two sensors. The Pearson correlation co-efficient shows a positive relation each with its own data. The 1150nm wavelength give good results it is apparent that 1150nm depicts higher sensitivity and high responsiveness to changes which is not depicted by 940nm.

Keywords: Blood Glucose Levels, Diabetes Management, Glucose Monitoring, Infrared Sensors, Non-Invasive Measurement, Optical Sensors,

INTRODUCTION

Globally, diabetes has increased alarmingly among many communities. The disease occurs when the body is not able to respond to insulin or when insulin is not sufficient in the body. The associated diseases that accompany diabetes are blindness, heart failure among others (Gayathri *et al.*, 2017: Hina *et al.*, 2019: Darwich *et al.*, 2023).

As per Ogurtsova *et al.*, (2017) the WHO's report of 2015 to 2040 estimate that 640 million people will suffer from diabetes by 2040. The death rate annually is approximated to be 5 million people. The approximated treatment cost for diabetes is Kshs 75 trillion (Ogunsanya and Daramola, 2022).

The prevalence rate of diabetes in Kenya is approximated to be 3.4% and it is estimated that by 2044, 500 thousand

people will be affected. The estimated individual cost of treatment is approximated to be Kshs 78,000 per person per year. This gives an approximate expenditure of about Kshs 38.5 billion (Oyando *et al.*, 2020).

In order to live with the disease, patients require to constantly monitor blood glucose, observe diet and use insulin as per the direction of the doctor. This necessitates routine blood glucose monitoring (Javid *et al.*, 2018).
The current methods used for routine glucose monitoring range from invasive to minimally invasive. The use of these techniques despite of their usefulness, are painful and in the long run, costly, stressful, and not free from infections (Sridevi *et al.*, 2021).

Currently, significant researches are underway on the establishment of non-invasive techniques for glucose measurement. These techniques may include Raman Spectroscopy, Fluorescence, Mid Infrared (MIR), Bio-impedance, and Near Infrared (NIR) Spectroscopy (Reddy and Jyostna, 2017: Feyikemi and Owoeye, 2024).

The use of NIR technique when compared with other non-invasive techniques give promising results. This is because NIR light can penetrate skin up to a depth of 1-100 mm which is easy to give results for medical examination. In addition, the components used to fabricate them are cheap, readily available, and that the method is pain free (Patel, 2017: Feyikemi and Owoeye, 2024).

In the pursuit to getting devices for monitoring glucose non-invasively, researches have encountered challenges that hinder full realization and commercialization of non-invasive glucose measuring devices (Tiberi *et al.*, 2016). These challenges have led to failure of realizing non-invasive glucose measuring devices that are suitable and viable (Saleh *et al.*, 2018: Al-Dhaheri *et al.*, 2020).

In order to address the challenge of in-accuracy, (Vanitha *et al.*, 2016) designed and developed a device that addresses estimation inaccuracies. The device had the capability of despising insulin automatically to hospitalized patients. Irrespective of the capabilities, the device is bulky and not adaptable. This is because it is exclusively designed for individuals who are bedridden (Vanitha *et al.*, 2016: Kalaivani *et al.*, 2020).

Furthermore, noise interferences as per Narkhede *et al.*, (2016) and Jernelv *et al.*, (2019) is another challenge that is hindering the realization of non-invasive glucose measuring devices. In order to solve the challenge of noise, , (Nanayakkara *et al.*, 2018) developed a hybrid system. The system used NIR technique and Bio-Impedance. The results gave an accuracy of 90% and 10% respectively. However, the system is prone to background light and it is also subjective because it is not user friendly (Nanayakkara *et al.*, 2018: Ali *et al.*, 2017).

Furthermore, and the use of indirect measurement and validation of the results is another challenge. It is established by (Surendran & Sasikala, 2019) that their 940nm NIR gave workable system. However, it required more validation in order to improve the system's accuracy and reliability (Surendran and Sasikala, 2019). In addition, Aswathy and Anusree, (2017) established that calibration methods also another challenge that affect the use of non-invasive glucose NIR techniques for monitoring glucose (Aswathy and Anusree, 2017: Jayarathan *et al.*, 2019).

The low sensitivity and low specificity as per (Gonzales *et al.*, 2019) are the other difficulties faced in the use of NIR methods (Gonzales *et al.*, 2019) Besides these, the invasive methods and minimally invasive methods currently in use have short sensor lifetime (Heo and Kim, 2019).

As per Kirui *et al.*, (2024), 1150nm wavelength present a possible way of non-invasively measuring glucose concentration. The system requires the use of in-vivo testing with large number of data set. It is to ensure validation and calibration with the comparison of presently used glucometers in order to increase system accuracy (Kirui *et al.*, 2024).

As an endeavor of establishing possible solutions to the existing challenges, the study sought to comparatively investigate 940nm and 1150nm NIR systems in order to ascertain their efficacy and suitability for measuring glucose non-invasively.

MATERIALS AND METHODS

Methods

In the research, the transmittance principle was adopted as per Beer-Lambert's law and all the conditions set were followed during the testing (Aryal. S, 2022: Calloway, 1997). This is illustrated in equation (1) and (2) (Haxha and Jhoja, 2016). Therefore, absorbance (A) is given by:

$$A = log\left(\frac{I_0}{I_t}\right) = \varepsilon ClA = log\left(\frac{I_0}{I_t}\right) = \varepsilon Cl \qquad (1)$$

where;
Ɛ=absorptivity, l=path length, C=concentration

Hence;

$$A \propto CA \propto C \qquad (2)$$

The equation (3) was used to calculate glucose concentrations for testing.

$$c_1v_1 = c_2v_2 \;\; c_1v_1 = c_2v_2 \quad (3)$$

Materials

In the experiment, 940nm and 1200 ± 50 nm IR LEDs were used as NIR light sources. These wavelengths were chosen because they fall among the peak points for glucose absorption, and therefore were suitable for use in glucose monitoring devices.

The detectors selected were photodiodes with spectral wavelengths ranging from 900nm to 1700nm and two photodiodes were used. These were chosen because they are able to receive NIR light source of 940nm and 1200nm wavelengths.

LM358 Op amp together with the feedback resistors were used to realize the current to voltage converter for both 1150nm and 940nm. The feedback resistors were 1 MΩ and 100 kΩ respectively together with 1nF capacitor in the feedback path. The output voltages were measured using the digital multi-meter.
The schematic diagram of the two systems were designed using the block diagram of Fig.1

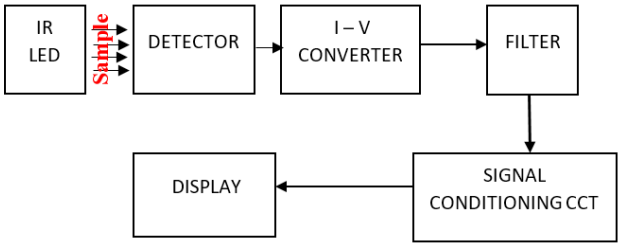

Fig.1. Block diagram for NIR glucose monitoring device

In the Fig. 1, the IR LED is a transmitter which emits IR light that passes through the sample for measurement. The photodiode upon detecting the IR light, transmit the photocurrent to the current to the trans-impedance amplifier to convert photocurrent into voltage. The output voltage is then filtered by the filter to remove noise interferences. The signal conditioning circuit consist of an amplifier to amplify the signal and a linearizer whose function is to linearize the signal to make it suitable for measurement.

RESULTS AND DISCUSSION

Table 1 shows the output voltages of 324ppm, 270ppm, 216ppm, 162ppm, 126ppm, 100.8ppm, 94.68ppm, 88.56ppm, 82.44ppm, 76.32ppm, 70.2ppm, 66.6ppmL, 63ppm, 59.4ppm, and 55.8ppm glucose concentration of 1150nm and 940nm IR sensors.

When the 1150nm IR light source and the photodiode were activated with no sample inserted in between, the current to voltage converter output was 600mV. When the distilled water is tested, the current to voltage converter output is 150mV.

When the 940nm IR sensor is activated with no sample in between the IR light source and the detector, the current to voltage converter output is 180mV. When distilled water is inserted in between the IR light source and the detector, the current to voltage converter output is 136 mV.

Table 1: Output Voltages for 1150nm and 940 nm wavelengths

Glucose Concentration (PPM)	Output Voltage (mV) ±5 (1150nm)	Output Voltage (mV) ±5 (940nm)
342	2110	950
270	2050	820
216	1520	650
162	1553	510
126	1315	330
100.8	1326	310
94.68	985	285
88.56	873	276
82.44	870	270
76.32	824	265
70.2	785	259
66.6	745	250
63	725	225
59.4	642	220
55.8	550	200

From the results, it is clear that water absorbance is minimum at 940nm and this is the reason why lower values were observed in air and water when compared to 1150nm IR sensor. It is also apparent that as glucose concentration increases, the voltage output also increases. This is illustrated in Figure 2.

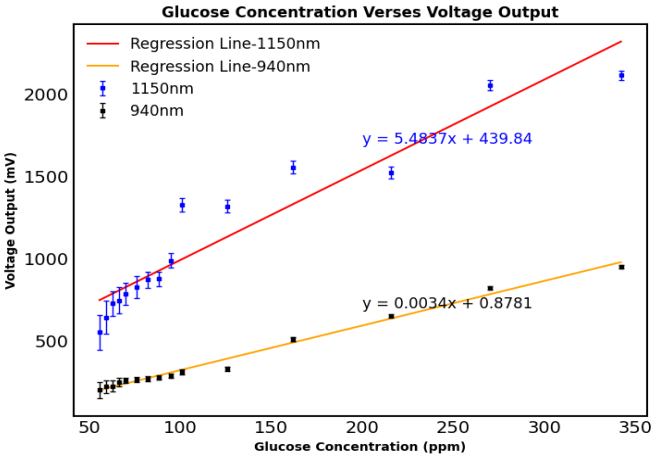

Fig. 2. Glucose concentrations Verse Voltage Output for 1150nm and 940nm

In Figure 2, a scatter plots for both 940nm and 1150nm NIR sensor output voltages against glucose concentration are plotted.

In Figure 2, it is observed that as glucose concentration increases, the voltage outputs for the two also increase similarly. Additionally, the output voltage range of 1150nm wavelength begins from 550mV to 2110mV. This shows a much wider span of output voltage when compared to the 940nm wavelength which begins from 200mV to 950mV. It indicates that 1150nm is much more responsive and covers a wider voltage output than 940nm. Despite these, there is less consistency of data points along the regression line in 1150nm wavelength when compared to the data points of 940nm wavelength which exhibit more consistency along the regression line. Irrespective of these variations, it is easily deducible that the two IR LEDs can detect glucose concentration non-invasively.

The voltage step changes give a pattern that is of importance in the analysis of the sensitivity and responsiveness of the two wavelengths. The different patterns that are observed from the two wavelengths (1150nm and 940nm) are from 55.8 ppm – 100.8 ppm and 126 ppm – 342 ppm glucose concentration. These are represented in Figure 3(a) and Figure 3(b) respectively.

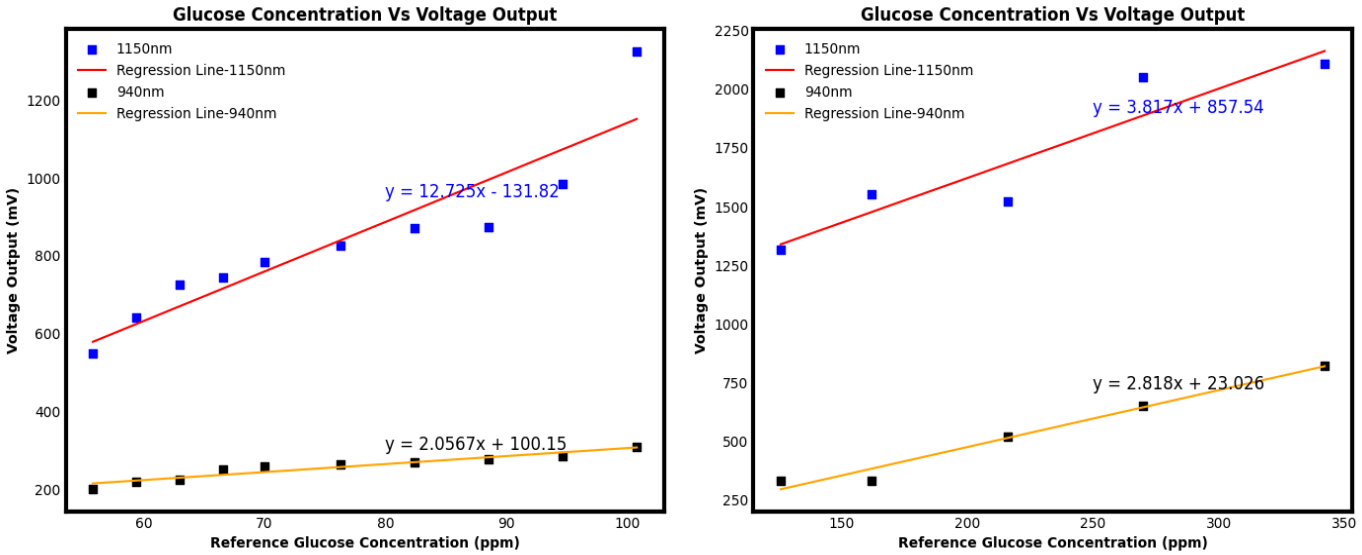

(a) Glucose concentrations from 55.8 ppm to 100.8 ppm

(b) Glucose Concentrations from 126 ppm to 342 ppm

Figure 3: Regression lines at different glucose concertation

Figure 3(a) illustrates a graph of glucose concentrations ranging from 55.8ppm to 100.8ppm. The voltage outputs appear to be more reliable and aligned with the regression lines in both wavelengths. The voltage step changes are smaller in both wavelengths and the data points around the regression lines show little variation, indicating that the prediction accuracy is relatively good at glucose concentration below 100.8ppm. Furthermore, the slope of the 1150nm wavelength is 12.725 which is steeper when compared to that of the 940nm wavelength which has a gradient of 2.0567. This suggests that 1150nm is more sensitive than 940nm. It is observed that at low and high glucose concentrations the voltage outputs appear to be more reliable and aligned with the regression lines for both wavelengths. The data points around the regression lines show little variation, indicating that the prediction accuracy is relatively good. Moreover, the regression lines for both wavelengths exhibit almost non-parallel slopes with different gradients. This indicates that the two wavelengths give a response to the changes in glucose concentrations and hence a clear and comparable relationship between reference glucose concentration and voltage outputs.

Figure 4(b) shows the graph of glucose concentrations ranging from 126ppm to 342ppm. It is seen that there is greater data variability and wider step changes in the voltage outputs and there is scattered data points around the regression lines for both wavelengths but the data points are scattered more for 1150nm when compared to that of 940nm. This increased variability can be attributed to factors such as indirect measurement and the limitations of the testing technique adopted. The slope of the 1150nm wavelength is slightly steeper with a gradient of 3.817 when compared to the slope of the 940nm wavelength which has a gradient of 2.818. This shows that 1150nm is more sensitive than 940nm.

It is apparent that at high glucose concentrations, there

is greater variability in the voltage outputs along the regression lines. This result in scattered data points around the regression lines for both wavelengths. The data points are more scattered around the regression line for 1150nm when compared to the data points for 940nm wavelength which are not much scattered along the regression line. Irrespective of the increased variability, the two wavelength's regression lines generally maintain almost parallel overall trends with different gradient; thus, indicating consistency in the relationship between reference glucose concentration and voltage outputs. Therefore, can detect the changes in glucose concentrations despite the wider spread and scattering along the regression lines.

The observations between low and high glucose concentrations from Fig.3 provide insights into the behavior and performance of the non-invasive glucose measurement technique at different sugar concentration levels. Additionally, the regression equation 2is fitted to the data of Figure 2 is used to predict measurements at one wavelength based on measurements at the other wavelength. Understanding these patterns help assess the method's reliability, identify potential limitations, and guide further investigation or refinement to optimize glucose measurement accuracy across the entire concentration range. By doing so, it is possible to determine if measurements made at one wavelength are predictable from measurements made at another. Therefore, the slope, range, and consistency of the regression lines for both 1150nm and 940nm sensors provide valuable insights into the responsiveness and performance of the two for measurement of glucose level. The following is therefore deducible from Figure 2.

Steepness of the Lines: The steepness of each line represents the rate at which the voltage output changes concerning the changes in glucose concentration. A steeper slope indicates a more sensitive sensor that produces larger changes in voltage output for small changes in glucose concentration. This is true for the 1150nm wavelength with a gradient of 12.725 when compared with 2.0567 for the 940nm wavelength.

Range of Voltage Output: It is clear that there is a spread of data points along each line. This indicates the range of glucose concentrations that each wavelength can detect. The 1150nm wavelength has a wider spread compared to 940nm. This depicts that the 1150nm sensor can sense a broader range of glucose concentrations as opposed to 940nm. It therefore demonstrates that 1150nm has greater responsiveness on a wider spectrum of glucose levels than 940nm. This is essential in the determination of the accuracy and reliability of 1150nm for glucose monitoring.

Consistency of Responsiveness: Consistency in the slope of the lines across different glucose concentrations indicates stable sensor responsiveness. In fig. 3, 940nm gives a consistent slope as opposed to 1150nm. It suggests that 940nm can maintain a predictable relationship between glucose concentration and voltage output when compared to 1150nm wavelength which does not give consistency but has a wide spread along the regression line. This is essential in the determination of the accuracy and reliability of glucose monitoring.

In view of the above, irrespective of the fact that 940nm shows consistency as opposed to 1150nm, it is apparent that 1150nm depicts higher sensitivity and high responsiveness to changes which is not depicted by 940nm. Therefore, the results above suggest that 1150nm wavelength gives good results and is likely to give a device that is more sensitive and more responsive subject to more validation and calibration that will enhance inconsistencies.

SYSTEM VALIDATION

Clarke Error Grid

The Clarke Error Grid is an analysis tool developed to quantify the clinical suitability of a new measurement device for use in glucose measurements. The Clark Error Grid plots measurements of the same variable on both x and y-axes. The reference measurements are set as per the WHO glucose sugar ranges. The reference glucose measurement is set to have similar scales with the measured glucose measurement. The glucose readings from the new device are superimposed onto the graph (Mondal & Mondal, 2020),. The grid is divided into five zones with each zone having its own judgment opinion. The zones are named A, B, C, D, and E. Region A is a zone where when values in that region - are 20% within the reference measurement, and region B is a region where values in that zone are 20% outside the reference measurement. The judgment in this zone is that data points here will not affect clinical decisions. Region C is a zone where values falling in the zone are not necessary and therefore not needed for clinical use. Region D is a region where values falling here are potentially dangerous and hence will mislead clinical treatment. Region E is the zone where values falling here will be confusing and will not be used for clinical treatment (Mondal & Mondal, 2020).

The Clarke error grid for 1150nm and 940nm were created side by side as shown in Figure 19 (a) and Figure 19(b) respectively to ascertain the suitability of the 1150nm device for glucose measurement and in comparing with the Clarke Error Grid for 940nm.

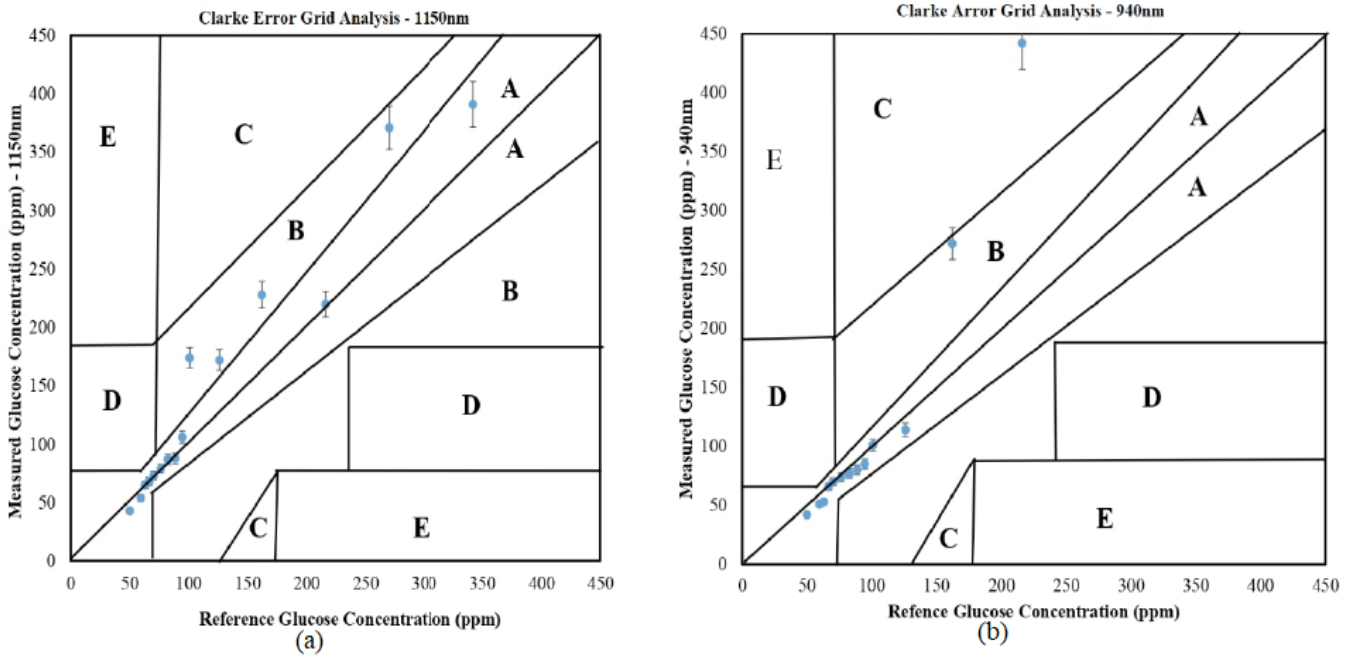

Figure 4: The graph of Clark Error Grid Analysis for 1150nm and 940nm

In representing the values of the 1150nm device onto the Clark Error Grid, it is observed that out of 15 measurements, region A has 11 data points which is 73% and region B has 4 data points which is 27% as indicated in Figure 4(a). It therefore informs that 11 values in region A are within 20% of the reference measurements and the 4 values in region B are 20% outside the reference measurement. All the data points are within region A and region B.

In representing the data points for the 940nm device onto the Clarke Error Grid, it is seen that out of the 15 measurements, region A has 13 data points which is 86.67%, region B has 1 data point which is 6.67%, and region C has 1 data point which is 6.67%. The data point in region C gives results that will not be necessary for use in non-invasive glucose treatment. The majority of the data points are falling in region A and region B.

In the above analysis, it is apparent from the analysis that the values of the 1150nm NIR meter are in region A and region B of the Clark Error Grid Analysis. It therefore indicates that the NIR meter developed is suitable for use to detect glucose concentration. This is because no values are falling on regions C, D, and E; hence increasing the efficacy of the 1150 NIR meter for use in non-invasive glucose measurement. On the other hand, it is observed that the 940nm wavelength despite having values of 86.67% and 6.67% in regions A and B respectively, it has values in region C. The values in the region Care not necessary to use in non-invasive glucose measurement. In examining the percentage concentration of data points in region A and region B, 1150nm has a higher percentage both in region A and B than the 940nm wavelength. Also, there is no data point in region C for 1150nm wavelength but there is a data point in region C for 940nm wavelength. Therefore, when the two wavelengths are compared; the 1150nm gives a greater suitability for glucose measurement than 940nm. This is because 1150nm has system have 100% of values in region A and B. The 940nm system have 93% of values in region A and B. These are regions where data are acceptable for clinical use. It suggests that 1150nm system give 100% of values for clinical use whereas 940nm system give 93% of values for clinical use.

Bland Altman Analysis

The Bland Altman's plot is one of the tools used to examine the agreements that occur between two measurement methods of the same variables (Giavarina, 2015) to determine the degree of accuracy. The limits of agreement constructed assist in quantifying the agreement between the two methods. The limits of agreement are arrived at by establishing the mean and the standard deviations of the two measurements' differences. Equation (4) was used to arrive at both the upper limit and the lower limits of agreements. A graphical approach is then employed in ascertaining the normality of the differences.

$$d \pm 1 \cdot 96 \times SD \quad (4)$$

where, d is the mean of the differences, SD is standard deviation.

As per (Hofman et al., 2015), 2015), it is recommended by Bland Altman that the data points plotted have to fall

within the upper limit and the lower limit of agreement for the measurement method to be 95% accurate. The Bland Altman analysis for both 1150nm and 940nm are illustrated in Figure 20 (a) and Figure 20 (b) respectively.

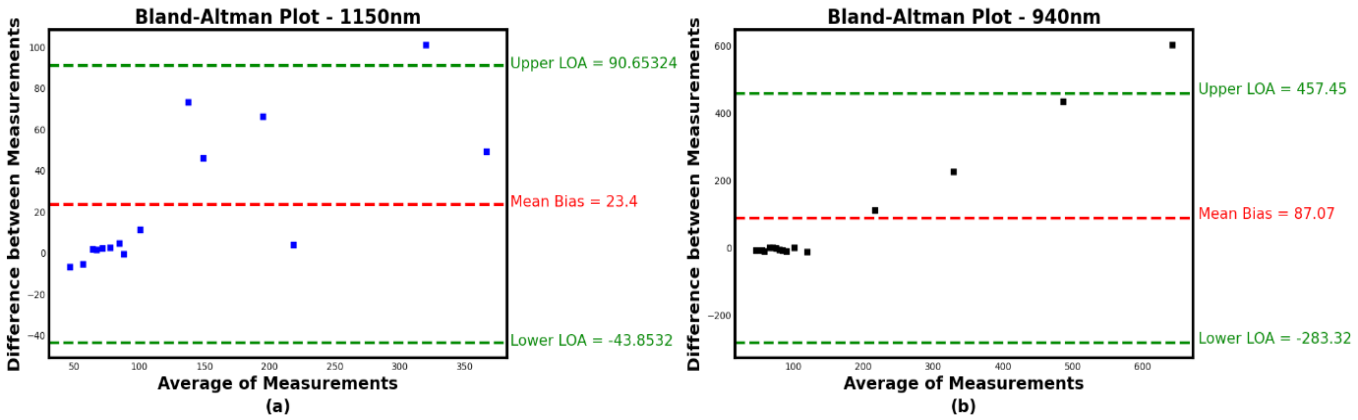

Figure 5: Bland Altman Analysis for 1150nm and 940nm

In observation from figure 5(a), that majority of the data points fall within both the upper and the lower limit of agreement, except one data point which is outside the upper limit of agreement. In figure 5(b), it is observed that majority of the data points are falling within the upper limit of agreement and lower limit of agreement except one data point which is falling outside the upper limit of agreement. In both cases, the degree of accuracy is 93.33%. Therefore, 1150nm and 940nm have the same degree of accuracy.

Residual Plot

The random scattering of data points around the zero line in a well-designed residual plot suggests that the residuals are randomly distributed and lack any discernible pattern. The residuals do not capture the underlying relationship between the variables if patterns or trends are observed (Kozak & Piepho, 2018). The residual plot for 1150nm and 940nm are given in figure 7 (a) and figure 7(b) respectively.

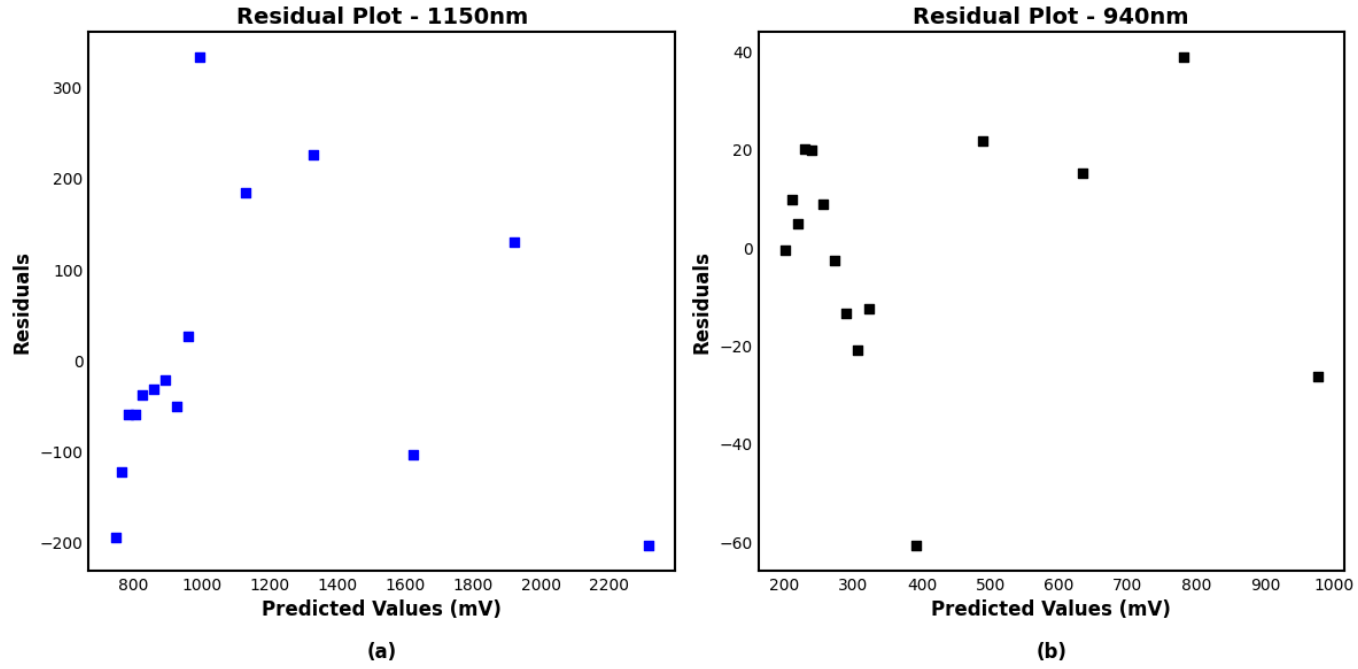

Figure 6: Residual plot for (a) and (b) wavelengths

The residual plot of Figure 6(a) and Figure 6(b) for the 1150 nm and 940nm data respectively shows no discernible trend, just a random spread of data points around the horizontal axis. This shows that for various levels of the predictor variable - reference glucose concentrations, the variance of the residuals is essentially constant. As such, it indicates that the homoscedasticity assumption is fulfilled, therefore, suggesting that the reference concentrations of

glucose do not have a systematic influence on the variation of the non-invasive sugar readings.

Additionally, from Figure 6(a) and Figure 6(b), there is no observable typical pattern for both 1150nm and 940nm respectively, such as funneling or curvature. The residuals' clear random distribution along the horizontal axis indicates that there is essentially a linear relationship between the non-invasive glucose readings and the reference glucose values. Therefore, based on the residual plot above, the linearity assumption appears to be reasonable.

Moreover, the residual plot lacks any noticeable outliers or pivotal points in both 1150nm and 940nm. Therefore, there appear to be no extreme observations that could adversely affect the regression model. This is because all of the data points are clustered within a reasonable range around the horizontal axis.

In view of this, the residual plot for the data at 1150 nm and 940nm indicates that the regression model adequately captures the relationship between the non-invasive glucose measurements and reference glucose concentrations. The absence of regular patterns, the random distribution of residuals, and the presence of outliers all suggest that the two models satisfy the requirements of linear regression and offer an acceptable fit to the data in each of them respectively.

Pearson Correlation Coefficient of 1150nm and 940nm

The Pearson correlation coefficient is a measure of the strength and direction of the linear relationship between two variables. It ranges from -1 to 1, as per (Chattamvelli, 2024), where 1 indicates a perfect positive linear relationship, -1 indicates a perfect negative linear relationship, and 0 indicates no linear relationship (Chattamvelli, 2024).

Equation (5) was used to calculate the person correlation coefficient for 1150nm and 940nm

$$r = \frac{\sum(x_i-\bar{x})(y_i-\bar{y})}{\sqrt{\sum(x_i-\bar{x})(y_i-\bar{y})}} \quad (5)$$

The Pearson correlation coefficient established for 1150nm and 940nm wavelength is 0.9894 and 0.9939 respectively. The 1150nm's Pearson correlation coefficient of 0.9894 indicates a nearly perfect positive linear relationship between the non-invasive glucose measurements with itself. This means that as one set of measurements increases, the other set also increases linearly, and vice versa. Essentially, the measurements at 1150nm are perfectly correlated with themselves, which is expected since it's the same dataset being compared to itself.

On the other hand, the 940nm's Pearson correlation coefficient of 0.9939 which is approximately 1.0 indicates a perfect positive linear relationship between the non-invasive glucose measurements with itself. It means that the measurements at 940nm are perfectly correlated with themselves, showing a consistent linear relationship within the dataset.

In both cases, the coefficients suggest a very strong positive linear relationship within each dataset, with the measurements depicting high consistency and predictability.

CONCLUSION

Within the two wavelengths two IR LEDs can detect glucose concentration non-invasively. Despite the fact that 940nm shows consistency as opposed to 1150nm, it is apparent that 1150nm depicts higher sensitivity and high responsiveness to changes which is not depicted by 940nm.

According to Clarke Error Grid Analysis, 1150nm and 940nm wavelength are suitable for non-invasive glucose measurements 1150nm indicating a higher efficacy because none of the data points are outside region and region B with region A (73%), region B (27%). The 940nm wavelength has data points in region A (86.67%), region B (6.67%), and C (6.67%).

As per Bland Altman analysis, the degree of accuracy in both is 93.33%. Therefore, 1150nm and 940nm have the same degree of accuracy.

In view of residual plot, the data for 1150 nm and 940nm indicates that the regression model adequately captures the relationship between the non-invasive glucose measurements and reference glucose concentrations. The absence of regular patterns, the random distribution of residuals, and the presence of outliers all suggest that the two models satisfy the requirements of linear regression and offer an acceptable fit to the data in each of them respectively.

The Pearson correlation coefficient for 1150nm and 940nm of 0.9894 and of 0.9939 respectively for 1150nm and 940nm respectively indicates a nearly perfect positive and a perfect positive linear relationship between the non-invasive glucose measurements with itself. In both cases, the coefficients suggest a very strong positive linear relationship within each dataset, with the measurements depicting high consistency and predictability.

ACKNOWLEDGMENT

We acknowledge the Department of Physics, Kenyatta University and the Department of Biological and Physical Sciences, Karatina University for their invaluable guidance and support during the research. In addition, we acknowledge Stephanie Wilsher, Joe Pullen, and Dawn Cook of Hamamatsu Photonics for their support during material selection, ordering, processing and ensuring that the crucial project materials were delivered safely.

Conflict of Interest

The authors declare that there were no conflicts of interest during the research and that none exist in the publication process of this paper.

Author Contributions

All authors contributed equally to the research at every stage. Julius Kirui developed the initial concept, while Mathew Munji, Raphael Nyenge, Lawrence Ochoo and John Okumu provided guidance, advice, and assistance throughout the concept development, implementation, final testing, and manuscript preparation.

REFERENCES

Al-Dhaheri, M. A., Mekkakia-Maaza, N. E., Mouhadjer, H., & Lakhdari, A. (2020). Noninvasive blood glucose monitoring system based on near-infrared method. *International Journal of Electrical and Computer Engineering*, *10*(2), 1736–1746. https://doi.org/10.11591/ijece.v10i2.pp1736-1746

Ali, H., Bensaali, F., & Jaber, F. (2017). Novel Approach to Non-Invasive Blood Glucose Monitoring Based on Transmittance and Refraction of Visible Laser Light. *IEEE Access*, *5*, 9163–9174. https://doi.org/10.1109/ACCESS.2017.2707384

Aryal. S. (2022). *Beer-Lambert Law- Definition, Derivation, and Limitations*. https://microbenotes.com/beer-lambert-law/

Aswathy S, & Anusree L. (2017). Non-Invasive Glucose Measurement Techniques using Near-Infrared Spectroscopy. In *International Journal of Innovative Science and Research Technology* (Vol. 2). www.ijisrt.com268

Calloway, D. (1997). Beer-Lambert Law. *Journal of Chemical Education*, *74*(7), 744. https://doi.org/10.1021/ed074p744.3

Chattamvelli, R. (2024). *Pearson's Correlation*. https://doi.org/10.1007/978-3-031-51015-1_2

Darwich, M. A., Shahen, A., Daoud, A., Lahia, A., Diab, J., & Ismaiel, E. (2023). Non-Invasive IR-Based Measurement of Human Blood Glucose †. *Engineering Proceedings*, *35*(1). https://doi.org/10.3390/IECB2023-14593

Feyikemi Owoeye, M., & Owoeye, A. B. (2024). Implementation of a real-time Arduino Based Non-Invasive Blood Glucose Monitoring System. In *International Journal of Advanced Academic Research* | (Vol. 10, Issue 2). www.ijaar.org

Gayathri, B., Sruthi, K., & Menon, K. U. (2017). *Proceedings of the 2017 IEEE International Conference on Communication and Signal Processing (ICCSP) : 6th-8th April, 2017, Melmaruvathur, India.* IEEE.

Giavarina, D. (2015). Understanding Bland Altman analysis. *Biochemia Medica*, *25*(2), 141–151. https://doi.org/10.11613/BM.2015.015

Gonzales, W. V., Mobashsher, A. T., & Abbosh, A. (2019). The progress of glucose monitoring—A review of invasive to minimally and non-invasive techniques, devices and sensors. In *Sensors (Switzerland)* (Vol. 19, Issue 4). MDPI AG. https://doi.org/10.3390/s19040800

Haxha, S., & Jhoja, J. (2016). Optical Based Noninvasive Glucose Monitoring Sensor Prototype. *IEEE Photonics Journal*, *8*(6). https://doi.org/10.1109/JPHOT.2016.2616491

Heo, Y. J., & Kim, S. H. (2019). Toward long-term implantable glucose biosensors for clinical use. In *Applied Sciences (Switzerland)* (Vol. 9, Issue 10). MDPI AG. https://doi.org/10.3390/app9102158

Hina, A., Nadeem, H., & Saadeh, W. (2019). A Single LED Photoplethysmography-Based Noninvasive Glucose Monitoring Prototype System. *2019 IEEE International Symposium on Circuits and Systems (ISCAS)*, *2019-May*, 1–5. https://doi.org/10.1109/ISCAS.2019.8702747

Hofman, C. S., Melis, R. J. F., & Donders, A. R. T. (2015). Adapted Bland-Altman method was used to compare measurement methods with unequal observations per case. *Journal of Clinical Epidemiology*, *68*(8), 939–943. https://doi.org/10.1016/j.jclinepi.2015.02.015

Javid, B., Fotouhi-Ghazvini, F., & Zakeri, F. (2018). Noninvasive optical diagnostic techniques for mobile blood glucose and bilirubin monitoring. *Journal of Medical Signals & Sensors*, *8*(3), 125. https://doi.org/10.4103/jmss.jmss_8_18

Jayarathan, M., Rajkumar, M., Sriraman, T., & Vetriselvan, V. (2019). GSM BASED NON-INVASIVE BLOOD GLUCOSE MEASUREMENT USING NEAR INFRARED SPECTROSCOPY. In *International Journal of Innovative Research in Advanced Engineering (IJIRAE)* (Vol. 6). www.ijirae.com

Jernelv, I. L., Milenko, K., Fuglerud, S. S., Hjelme, D. R., Ellingsen, R., & Aksnes, A. (2019). A review of optical methods for continuous glucose monitoring. In *Applied Spectroscopy Reviews* (Vol. 54, Issue 7, pp.

543–572). Taylor and Francis Inc. https://doi.org/10.1080/05704928.2018.1486324

Kalaivani, V., Arulladakanthan, & Arulvallal, S. (2020). Designing and Implementation of Non Invasive Blood Glucose and Hemoglobin Detection using NIR. *International Journal of Innovative Technology and Exploring Engineering*, *9*(12), 229–232. https://doi.org/10.35940/ijitee.K7768.0991120

Kirui, J., Mathew K. Munji, & Raphael L Nyenge. (2024). Advancing Glucose Monitoring: A Near-Infrared Device for Continuous Non-Invasive Assessment. *Andalas Journal of Electrical and Electronic Engineering Technology*, *4*(1), 8–14. https://doi.org/10.25077/ajeeet.v4i1.96

Kozak, M., & Piepho, H. P. (2018). What's normal anyway? Residual plots are more telling than significance tests when checking ANOVA assumptions. *Journal of Agronomy and Crop Science*, *204*(1), 86–98. https://doi.org/10.1111/jac.12220

Mondal, H., & Mondal, S. (2020). Clarke Error Grid Analysis on Graph Paper and Microsoft Excel. In *Journal of Diabetes Science and Technology* (Vol. 14, Issue 2, p. 499). SAGE Publications Inc. https://doi.org/10.1177/1932296819890875

Nanayakkara, N. D., Munasingha, S. C., & Ruwanpathirana, G. P. (2018). *MERCon 2018 : 4th International Multidisciplinary Engineering Research Conference : May 30-June 1, 2018, Civil Engineering Complex, University of Moratuwa, Sri Lanka*.

Narkhede, P., Dhalwar, S., & Karthikeyan, B. (2016). NIR based non-invasive blood glucose measurement. *Indian Journal of Science and Technology*, *9*(41). https://doi.org/10.17485/ijst/2016/v9i41/98996

Ogunsanya, A. O., & Daramola, D. O. (2022). Design and Development of a Non-invasive Glucometer System. *West Indian Journal of Engineering*, *44*(2), 70–79. https://doi.org/10.47412/icpw8648

Ogurtsova, K., da Rocha Fernandes, J. D., Huang, Y., Linnenkamp, U., Guariguata, L., Cho, N. H., Cavan, D., Shaw, J. E., & Makaroff, L. E. (2017). IDF Diabetes Atlas: Global estimates for the prevalence of diabetes for 2015 and 2040. *Diabetes Research and Clinical Practice*, *128*, 40–50. https://doi.org/10.1016/j.diabres.2017.03.024

Oyando, R., Njoroge, M., Nguhiu, P., Sigilai, A., Kirui, F., Mbui, J., Bukania, Z., Obala, A., Munge, K., Etyang, A., & Barasa, E. (2020). Patient costs of diabetes mellitus care in public health care facilities in Kenya. *International Journal of Health Planning and Management*, *35*(1), 290–308. https://doi.org/10.1002/hpm.2905

Patel, H. J. (2017). Near Infrared Spectroscopy: Basic principles and use in tablet evaluation. *International Journal of Chemical and Life Sciences*, *6*(2), 2006. https://doi.org/10.21746/ijcls.2017.2.1

Reddy, P. S., & Jyostna, K. (2017). *Development of Smart Insulin Device for Non Invasive Blood Glucose Level Monitoring*. https://doi.org/10.1109/IACC.2017.193

Saleh, G., Alkaabi, F., Al-Hajhouj, N., Al-Towailib, F., & Al-Hamza, S. (2018). Design of non-invasive glucose meter using near-infrared technique. *Journal of Medical Engineering and Technology*, *42*(2), 140–147. https://doi.org/10.1080/03091902.2018.1439114

Sridevi, P., Arefin, S., & Shahadat, A. (2021). A Feasibility Study of Non-invasive Blood Glucose Level Detection Using Near-Infrared Optical Spectroscopy. In *Bangladesh Journal of Medical Physics* (Vol. 14, Issue 1).

Surendran, K. S., & Sasikala, T. (2019). *Proceedings of the 3rd International Conference on Computing Methodologies and Communication (ICCMC 2019) : 27-29, March 2019*. IEEE.

Tiberi, E., Cota, F., Barone, G., Perri, A., Romano, V., Iannotta, R., Romagnoli, C., & Zecca, E. (2016). Continuous glucose monitoring in preterm infants: evaluation by a modified Clarke error grid. *Italian Journal of Pediatrics*, *42*(1), 29. https://doi.org/10.1186/s13052-016-0236-9

Vanitha, M., Mathew, G., Divya, K. S., & Vignesh, R. (2016). Non-Invasive Glucose Estimation Using IR Spectroscopy. *International Journal of Scientific and Research Publications*, *6*(5), 217. www.ijsrp.org